Hindawi
International Journal of Optics
Volume 2021, Article ID 6610674, 6 pages
https://doi.org/10.1155/2021/6610674

Research Article

Simultaneous Measurement of Distributed Temperature and Strain through Brillouin Frequency Shift Using a Common Communication Optical Fiber

Leijun Hu,[1] Liwen Sheng,[1,2,3,4] Jisong Yan,[1] Ligong Li,[1] Ming Yuan,[1] Fude Sun,[1] Fushun Nian,[2,4] Long Li,[3] Jiaqing Liu,[1,4] Shuai Zhou,[1] and Zhiming Liu[1]

[1]*Ceyear Technologies Co., Ltd, Qingdao 266555, China*
[2]*The 41st Institute of CETC, Qingdao 266555, China*
[3]*Xidian University, Xi'an 710071, China*
[4]*Science and Technology on Electronic Test & Measurement Laboratory, Qingdao 266555, China*

Correspondence should be addressed to Liwen Sheng; shengliwen2008@163.com and Jiaqing Liu; jiaqing@mail.ustc.edu.cn

Received 6 February 2021; Accepted 22 April 2021; Published 29 April 2021

Academic Editor: Zhenao Bai

A multiparameter Brillouin fiber-optic sensor for distributed strain and temperature information measuring based on spontaneous scattering in a common communication optical fiber (the G. 652. D commercial fiber) is presented and experimentally demonstrated. Benefiting from the difference of the temperature and strain sensitivity from different Brillouin peaks with different acoustic modes, our proposed sensing configuration can be used to distinguish ambient temperature and applied strain at the same time, which is an excellent candidate to address the problem of cross-sensitivity in the classical Brillouin system. In the experimental section, using a 21.8 km sensing length of communication optical fiber, a temperature accuracy of 1.13°C and a strain accuracy of 21.46 $\mu\varepsilon$ are obtained simultaneously. Considering the performance we achieved now, the proposed innovation and experimental setup will have some potential applications in the field of fiber sensors.

1. Introduction

Distributed optical fiber sensors, with the characters of long-haul and measuring environmental variables (e.g., temperature, strain, and vibrations), have been extensively investigated recently for sensing applications in nondestructive health monitoring of engineering facilities [1–4], human body motion detection [5], and geotechnical engineering [6]. Compared with traditional electrical sensing systems, the fiber-distributed sensing network provides an interesting solution due to the following main advantages: low cost, compactness, high sensitivity, immunity to external-electromagnetic interference, intrinsic chemical inertness, and long sensing range, where the fiber simultaneously serves as the interrogate signal transmission medium and a large number of closely spaced sensing points. To date, many different technologies have been developed, including Raman distributed temperature sensor (RDTS) [7, 8], Brillouin reflectometers (optical correlation domain (BOCDR), optical frequency domain (BOFDR), optical time domain (BOTDR)) [9–14], Brillouin analyzers (BOCDA, BOFDA, and BOTDA) [15–17], and Rayleigh reflectometer (optical frequency domain (OFDR)) [18]. Among these techniques, BOTDR, which is based on the spontaneous Brillouin scattering (SpBS) effect, is considered as one of the most potential sensing techniques that can simultaneously retrieve distributed temperature and strain information by single-ended fiber under test (FUT) architecture and random accessibility. This sensing technique relies on the measurement of the values of Brillouin frequency shift (BFS) along the sensing FUT to demodulate its strain and temperature information. However, the BFS in a distributed Brillouin scattering-based fiber-optic sensor has been demonstrated to depend on the combination of strain

and temperature characteristic changes since 1993 [19]. Since then, many novel methods have been presented to address this temperature and strain cross-sensitivity problem in the past few years. Bao et al. [20] apply half of the fiber as a reference to separate the effects of strain for temperature measurement. Davis et al. [21] report a Brillouin sensing element based on the integration of fiber Bragg gratings (FBG) and the FUT. Meanwhile, some researchers combine stimulated Brillouin scattering (SBS) with other nonlinear effects, for example, stimulated Raman scattering (SRS) to address this cross-sensitivity problem by temperature compensation [12, 22]. Other researchers demonstrate a multiparameter measuring device based on the stimulated scattering effect with loop architecture by means of the multicore optical fiber (MCF) to separate the temperature and strain individual contributions to the BFS of FUT by measuring the Brillouin gain spectra (BGSs) in different channels of FUT cores [23]. Recently, Xing et al. [24] apply the G. 652. D commercial fiber as a sensing element based on the SBS effect to eliminate the crosstalk caused by temperature and strain. It is evident that the methods mentioned above require rather complex measuring configurations.

In addition, an effective technique for the temperature and strain information recovery using multiple optical modes in the few-mode fiber (FMF) is proposed by Li et al. [25] in 2015. The few-mode fiber can contribute two BFSs at least. In the same year, Xu et al. [26] demonstrate a proof-of-concept multiparameter Brillouin-based optical fiber sensing idea based on the SBS effect. In their proposed scheme, an orbital angular momentum (OAM) guiding fiber with higher order acoustic modes is employed as FUT. The couplings of the guided modes and acoustic modes lead to the generation of the multipeak BGS of the OAM fiber. By choosing any two Brillouin peaks in the measured BGS, the reported unique method is able to demodulate distributed temperature and strain information along the FUT at the same time. Nevertheless, the radiation sources generally operate in fundamental mode, and it is going to bring extratechnical difficulties in transforming the fundamental mode into the desired pattern. In view of the above-proposed methods, using common communication optical fiber (G. 652. D) with multiple Brillouin peaks as the sensing medium is of great importance to realize the uncomplicated fiber-optic sensor networks with low cost. Meanwhile, combining the distributed sensing with communication optical fiber using a BFS demodulation, an SpBS sensor-based communication optical fiber for simultaneous temperature and strain monitoring can be developed. Therefore, it is a good alternative to satisfy the practical engineering applications.

Here, a multiparameter Brillouin sensor is proposed and experimentally demonstrated, which utilizes a common communication fiber having multipeak, corresponding to multiple acoustic modes, with unequal Brillouin gain coefficients in the core to simultaneously monitor the temperature and strain information based on the SpBS effect. This presented method only requires measuring the central frequency shifts of the Brillouin spectra and can simultaneously accomplish the temperature and strain information measurement without replacing the FUT. Moreover, the corresponding results also indicate that the reported method is suitable to realize simultaneously temperature and strain sensing in a relatively uncomplicated single-end configuration, and a measurement accuracy of 21.46 $\mu\varepsilon$ and 1.13°C is exhibited in the 21.8 km sensing range, respectively.

2. Theory

The BFS of measured fiber depends heavily on the inherent refractive index (RI) n, the acoustic velocity V_a, and the central wavelength of incident probe wave λ. For a common communication optical fiber at room temperature ($T = 20$°C), the BFS is about 11 GHz when λ is 1550 nm [27]. Based on a previous theoretical analysis, in the case of a FUT with multiple acoustic modes, n and V_a vary with the variation of temperature ΔT or strain $\Delta\varepsilon$. The change of BFS related to ΔT and $\Delta\varepsilon$ can be described by the following formula:

$$\begin{pmatrix} \Delta\nu_B^1 \\ \vdots \\ \Delta\nu_B^m \end{pmatrix} = \begin{pmatrix} C_T^1 & C_\varepsilon^1 \\ \vdots & \vdots \\ C_T^m & C_\varepsilon^m \end{pmatrix} \begin{pmatrix} \Delta T \\ \Delta\varepsilon \end{pmatrix}, \tag{1}$$

where C_ε^m and C_T^m are the Brillouin gain coefficients (e.g., strain and temperature) of the m-order acoustic mode in the G. 652. D, respectively. $\Delta\nu_B^m$ denotes the movement of BFS caused by the contribution of the m-order acoustic mode.

Consequently, the changes of temperature and strain sensing information can be derived from equation (1), described as the following formulas:

$$\begin{aligned} \Delta T &= \frac{C_\varepsilon^m \Delta\nu_B^1 - C_\varepsilon^1 \Delta\nu_B^m}{C_T^1 C_\varepsilon^m - C_T^m C_\varepsilon^1}, \\ \Delta\varepsilon &= \frac{C_T^1 \Delta\nu_B^m - C_T^m \Delta\nu_B^1}{C_T^1 C_\varepsilon^m - C_T^m C_\varepsilon^1}. \end{aligned} \tag{2}$$

Obviously, the proposed method with multiple acoustic modes in common communication optical fiber-based on Brillouin scattering has the ability to solve the cross-sensitivity problem along the whole sensing link via the frequency analysis of the monitored Brillouin spectra. In addition, the measurement error analysis of temperature and strain can be described as [28]

$$\delta T = \frac{\left|C_\varepsilon^m\right|\delta\nu_B^1 + \left|C_\varepsilon^1\right|\delta\nu_B^m}{\left|C_T^1 C_\varepsilon^m - C_T^m C_\varepsilon^1\right|}, \tag{3}$$

$$\delta\varepsilon = \frac{\left|C_T^1\right|\delta\nu_B^m + \left|C_T^m\right|\delta\nu_B^1}{\left|C_T^1 C_\varepsilon^m - C_T^m C_\varepsilon^1\right|}. \tag{4}$$

3. Experimental Setup

Based on the above theoretical analysis, an experimental arrangement is built as depicted in Figure 1. The continuous-wave probe light from a 13 dBm, 10 kHz linewidth, 1550 nm wavelength distributed feedback laser (DFB) is divided into two branches by a coupler (OC1, 90 : 10) for the generation of

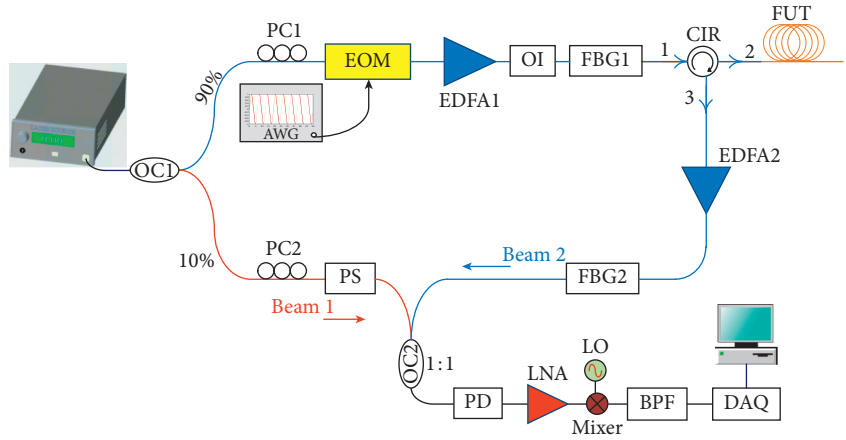

Figure 1: Schematic diagram of experimental apparatus. OI: optical isolator; OC: optical coupler; BPF: band-pass filter; PS: polarization scrambler; AWG: arbitrary waveform generator; PD: photodetector; DAQ: data acquisition card; EOM: electro-optic modulator; EDFA: erbium-doped fiber amplifier; FUT: fiber under test; FBG: fiber Bragg grating; CIR: circulator; LNA: low-noise amplifier; LO: local oscillator; PC, polarization controller.

Brillouin backscattering signal (beam 2) and reference light signal (beam 1). The upper branch is launched into the customized electro-optic modulator (EOM: iXblue, MXER-LN-20) with 40 dB high extinction ratio to generate 30 ns Gaussian probe pulses. The 30 ns pulse width indicates that the spatial resolution is about 3 m. The customized EOM is driven by an arbitrary waveform generator (AWG). The modulated pulse is amplified by an erbium-doped fiber amplifier (EDFA1) and then injected into the measured FUT with 21.8 km in length through an optical circulator (CIR). The 10% optical coupler enables us to monitor the input continuous-wave power to the heterodyne detection stage. The lower branch is reserved as beam 1 to perform coherent detection. Furthermore, since the beat intensity is heavily related to the state of polarization (SOP) of beam 1 and beam 2, we scramble beam 1 polarization using a polarization scrambler (PS) to eliminate the fading noise of polarization [29]. The weak Brillouin backscattering sensing signal from the third port of the CIR is amplified by EDFA2. Two-fiber Bragg grating (FBG) optical filters (FBG1 and FBG2) are used to prevent further propagation of the parasitic light spontaneously emitted by EDFA1 and EDFA2, respectively. Finally, beam 2 and beam 1 are mixed through a 3 dB coupler (OC2), and then the Brillouin beat signals are converted into electrical signals with a 13.5 GHz photodetector (PD). The captured electrical signals are boosted by a low-noise amplifier (LAN). The enhanced sensing signal is downconverted by mixing with a local oscillator (LO). The frequency sweeping is achieved by adjusting the output frequency of the LO. The intermediate frequency signals filtered by a band-pass filter (BPF) are received by a logarithmic detector and eventually sampled by a data acquisition (DAQ) card for follow-up data processing to accomplish the strain and temperature information demodulation.

3.1. Experimental Results and Discussion. A common communication optical fiber is adopted to retrieve the strain and temperature sensing information, which is fabricated in Yangtze Optical Fiber Cable Co., Ltd. (YOFC, PH1010-A). It is noteworthy that the fabrication process and doping concentration of the G. 652. D will be slightly different from each other in different manufactures. Therefore, the corresponding experimental results may be different. The BGS distribution along the entire length of the FUT is measured to obtain the BFS, and its response to surrounding environmental temperature and strain is characterized, respectively.

The measured three-dimensional map of the gain spectrum along the communication optical fiber at room temperature (26°C) is highlighted in Figure 2(a), where red denotes a higher Brillouin amplification factor. Figure 2(b) illustrates the distribution of the measured BGS along the FUT, where an increase in BFS at the heating region can be discovered. As Figure 2 shows, the central frequencies of three Brillouin peaks are 10.875 GHz, 11.020 GHz, and 11.115 GHz for peaks 1–3, respectively. Consequently, the frequency shift of different Brillouin peaks in communication optical fiber could be calculated by monitoring the BGS at different environmental conditions. As described in Section 2, taking advantage of the communication optical fiber (G. 652. D) with multipeaks, a distributed simultaneous strain and temperature measuring device is able to be developed, which is based on multiple acoustic modes in spontaneous scattering effect. For the temperature coefficients measurement, a 5 m segment at the far end is immersed in a temperature-controlled water-bath pot (JOANLAB, HH-2), and the temperature is increased from 40°C to 80°C with 10°C per step. Remarkably, the length of the heated segment is about 5 m which is longer than the spatial resolution (3 m). In order to effectively eliminate the influence of crosstalk, the strain remains unchanged when the temperature coefficients are monitored. The BGSs of the communication optical fiber under different temperatures are measured and drawn in Figure 3. Meanwhile, the Lorentz fitting based on the least-squares method is applied to the measured BGS.

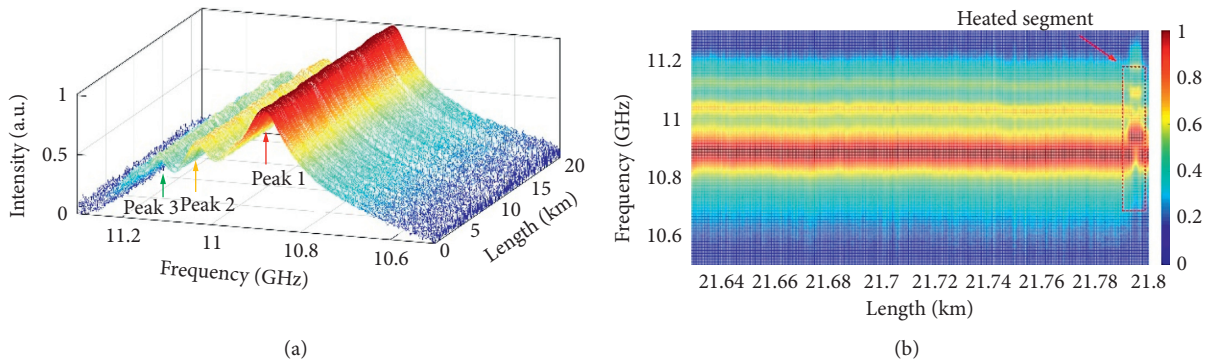

(a) (b)

Figure 2: (a) Three-dimensional map of the measured Brillouin gain spectrum as a function of length and (b) measured Brillouin gain spectrum with a heated segment.

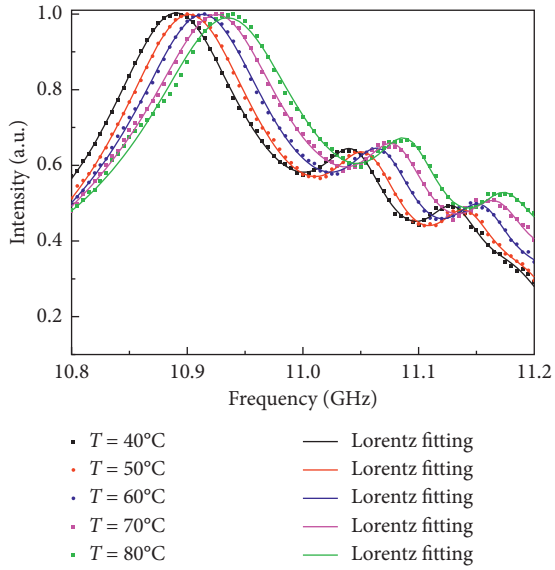

Figure 3: Measured Brillouin gain spectra of multipeak under different temperatures with a step of 10°C.

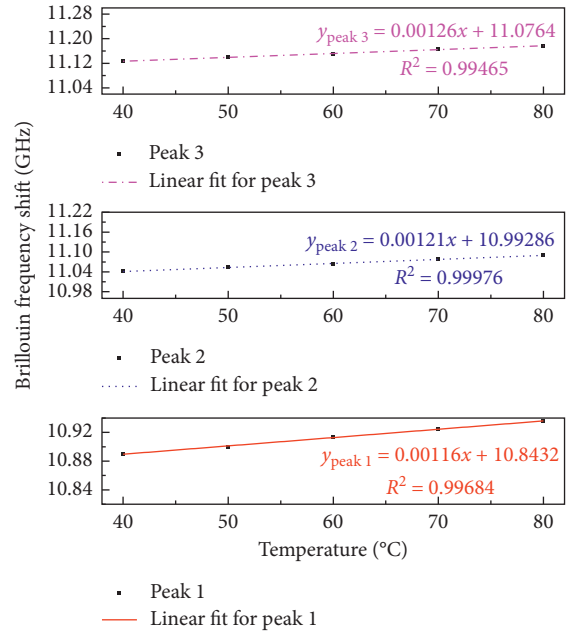

Figure 4: Measured BFS as a function of temperature for peak 1, peak 2, and peak 3, respectively.

As shown in Figure 3, when the ambient temperature is changed, the gain spectrum also changes and moves to a higher frequency with the increase of the ambient temperature. Even more importantly, the gain spectrum of the other Brillouin peaks also shifts to a higher frequency at the same time, although the gain factor is smaller than the first Brillouin peak (or called main peak). From the data, the temperature coefficients of the BFS C_T^1, C_T^2, and C_T^3 are determined to be 1.16 MHz/°C, 1.21 MHz/°C, and 1.26 MHz/°C, respectively, by the linear fitting method as plotted in Figure 4.

Figure 5 highlights the measured sensing results of the communication optical fiber (~21.8 km) through a home-made single-ended network at room temperature (26°C). The FUT to be measured is applied to the axial strain by means of gradually changing the linear stage with 200 $\mu\varepsilon$ per step, and the stressed location of the sensing FUT is about 5 m. The BFSs can be obtained through the same procedure as mentioned above. The results of data analyzing proved that the strain sensitivities of the BFS, C_ε^1, C_ε^2, and C_ε^3 are determined to be 64.64 kHz/$\mu\varepsilon$, 50.96 kHz/$\mu\varepsilon$, and 42.76 kHz/$\mu\varepsilon$, respectively. Owing to the difference of strain and temperature coefficients of the three Brillouin peaks in the measured FUT, the influence of the cross-sensitivity on the FUT can be simultaneously discriminated. All of this is due to the different acoustic modes in the core. Meanwhile, the measurement accuracy of temperature and strain is solved by equations (3) and (4). With the help of the experimental data of the first two Brillouin peaks with a high signal-to-noise ratio in Figures 4 and 5, the respective errors of temperature and strain are calculated as 1.13°C and 21.46 $\mu\varepsilon$, respectively. Compared with the sensing system using a few-mode fiber as the measured FUT, the discrimination accuracy of the two sensing systems is similar [25]. Considering that the multiple Brillouin peaks can be easily achieved when the mode of the incident light is a fundamental mode. Hence, the sensing scheme seems to be simple and more conducive to large dynamic distributed sensing.

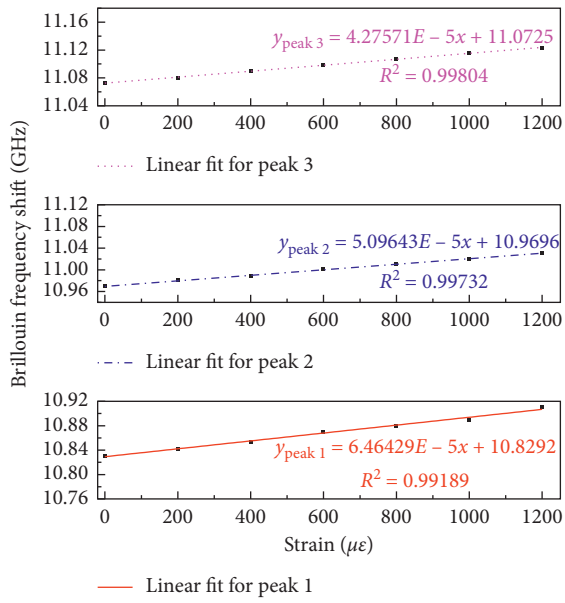

Figure 5: Measured BFS as a function of strain for peak 1, peak 2, and peak 3, respectively.

4. Conclusions

Here, a novel method to realize simultaneously the distributed strain and temperature monitoring is presented based on spontaneous scattering effect, which utilizes a common communication fiber having multipeak, corresponding to multiple acoustic modes, with unequal Brillouin gain coefficients in the core. Benefiting from the difference of the temperature and strain sensitivity from different Brillouin peaks with different acoustic modes, the simultaneous demodulation of strain and temperature information is successfully demonstrated with a strain accuracy of 21.46 $\mu\varepsilon$ and a temperature accuracy of 1.13°C in 21.8 km measuring range. And, we believe that the proposed innovation and experimental setup, with its excellent performances, will have some potential applications in the field of nuclear facilities and superconducting cables in the future. Besides, more than two Brillouin peaks are selected by rational optimization, and the presented method has the ability to be applied to multiparameter measuring situations where more than two parameters are required to be distinguished.

Data Availability

The data used to support the findings of this study have not been made available because our group is a confidential unit, and the experimental data are mainly used for the development of related instruments.

Conflicts of Interest

The authors declare that they have no conflicts of interest.

Acknowledgments

The authors gratefully acknowledge the financial support provided by the Science and Technology on Electronic Test and Measurement Laboratory Foundation (Grant no. 41Q1313-5 and KDW03012003), the Taishan Series Talent Project (Grant no. 2017TSCYCX-05), and the National Natural Science Foundation of China (Grant no. 61901426).

References

[1] X. Bao and L. Chen, "Recent progress in Brillouin scattering based fiber sensors," *Sensors*, vol. 11, no. 4, pp. 4152–4187, 2011.

[2] X. Bao and L. Chen, "Recent progress in distributed fiber optic sensors," *Sensors*, vol. 12, no. 7, pp. 8601–8639, 2012.

[3] P. Xu, Y. Dong, D. Fu et al., "1200°C high-temperature distributed optical fiber sensing using Brillouin optical time domain analysis," *Applied Optics*, vol. 55, no. 21, pp. 5471–5478, 2016.

[4] P. Xu, D. Ba, W. He, H. Hu, and Y. Dong, "Distributed Brillouin optical fiber temperature and strain sensing at a high temperature up to 1000 °C by using an annealed gold-coated fiber," *Optics Express*, vol. 26, no. 23, pp. 29724–29734, 2018.

[5] J. Guo, M. Niu, and C. Yang, "Highly flexible and stretchable optical strain sensing for human motion detection," *Optica*, vol. 4, no. 10, pp. 1285–1288, 2017.

[6] Z. He, Q. Liu, and T. Tokunaga, "Ultrahigh resolution fiber-optic quasi-static strain sensors for geophysical research," *Photonic Sensors*, vol. 3, no. 4, pp. 295–303, 2013.

[7] M. A. Soto, T. Nannipieri, A. Signorini et al., "Raman-based distributed temperature sensor with 1 m spatial resolution over 26 km SMF using low-repetition-rate cyclic pulse coding," *Optics Letters*, vol. 36, no. 13, pp. 2557–2559, 2011.

[8] C. Cangialosi, Y. Ouerdane, S. Girard et al., "Development of a temperature distributed monitoring system based on Raman scattering in harsh environment," *Institute of Electrical and Electronics Engineers Transactions on Nuclear Science*, vol. 61, no. 6, pp. 3315–3322, 2014.

[9] Y. Mizuno, W. Zou, Z. He, and K. Hotate, "Proposal of Brillouin optical correlation-domain reflectometry (BOCDR)," *Optics Express*, vol. 16, no. 16, pp. 12148–12153, 2008.

[10] A. Minardo, R. Bernini, and L. Zeni, "Stimulated Brillouin scattering modeling for high-resolution, time-domain distributed sensing," *Optics Express*, vol. 15, no. 16, pp. 10397–10407, 2007.

[11] L. Sheng, L. Li, L. Liu, L. Hu, M. Yuan, and J. Yan, "Study on the simultaneous distributed measurement of temperature and strain based on Brillouin scattering in dispersion-shifted fiber," *OSA Continuum*, vol. 3, no. 8, pp. 2078–2085, 2020.

[12] D. Ba, B. Wang, T. Li, Y. Li, D. Zhou, and Y. Dong, "Fast Brillouin optical time-domain reflectometry using the optical chirp chain reference wave," *Optics Letters*, vol. 45, no. 19, pp. 5460–5463, 2020.

[13] L. W. Sheng, L. G. Li, L. J. Hu et al., "Distributed fiberoptic sensor for simultaneous temperature and strain monitoring based on Brillouin scattering effect in polyimide-coated fibers," *International Journal of Optics*, vol. 2020, Article ID 8810986, , 2020.

[14] P. B. Xu, C. Pang, X. Y. Dong et al., "Fast acquirable Brillouin optical time-domain reflectometry based on bipolar-chirped pulse pair," *Journal of Lightwave Technology*, vol. 99, Article ID 3042237, 2020.

[15] D. W. Zhou, Y. K. Dong, B. Z. Wang et al., "Single-shot BOTDA based on an optical chirp chain probe wave for distributed ultrafast measurement," *Light: Science & Applications*, vol. 7, no. 1, p. 32, 2018.

[16] D. Ba, Y. Li, J. Yan, X. Zhang, and Y. Dong, "Phase-coded Brillouin optical correlation domain analysis with 2-mm resolution based on phase-shift keying," *Optics Express*, vol. 27, no. 25, pp. 36197–36205, 2019.

[17] R. Bernini, A. Minardo, and L. Zeni, "Distributed sensing at centimeter-scale spatial resolution by BOFDA: measurements and signal processing," *Institute of Electrical and Electronics Engineers Photonics Journal*, vol. 4, no. 1, pp. 48–56, 2012.

[18] Z. Ding, C. Wang, K. Liu et al., "Distributed optical fiber sensors based on optical frequency domain reflectometry: a review," *Sensors*, vol. 18, no. 4, Article ID 4, 2018.

[19] T. Kurashima, T. Horiguchi, H. Izumita, S. Furukawa, and Y. Koyamada, "Brillouin optical-fiber time domain reflectometey," *IEICE Transactions on Communications*, vol. E76-B, no. 4, pp. 382–390, 1993.

[20] X. Bao, D. J. Webb, and D. A. Jackson, "32-km distributed temperature sensor based on Brillouin loss in an optical fiber," *Optics Letters*, vol. 18, no. 18, pp. 1561–1563, 1993.

[21] M. A. Davis and A. D. Kersey, "Simultaneous measurement of temperature and strain using fibre Bragg gratings and Brillouin scattering," *IEE Proceedings-Optoelectronics*, vol. 144, no. 3, pp. 151–155, 1997.

[22] Z. Bai, H. Yuan, Z. Liu et al., "Stimulated Brillouin scattering materials, experimental design and applications: a review," *Optical Materials*, vol. 75, pp. 626–645, 2018.

[23] Y. Mizuno, N. Hayashi, H. Tanaka, Y. Wada, and K. Nakamura, "Brillouin scattering in multi-core optical fibers for sensing applications," *Scientific Reports*, vol. 5, no. 1, Article ID 11388, 2015.

[24] C. Xing, C. Ke, Z. Guo et al., "Distributed multi-parameter sensing utilizing Brillouin frequency shifts contributed by multiple acoustic modes in SSMF," *Optics Express*, vol. 26, no. 22, pp. 28793–28807, 2018.

[25] A. Li, Y. Wang, J. Fang, M.-J. Li, B. Y. Kim, and W. Shieh, "Few-mode fiber multi-parameter sensor with distributed temperature and strain discrimination," *Optics Letters*, vol. 40, no. 7, pp. 1488–1491, 2015.

[26] Y. P. Xu, M. Q. Ren, Y. Lu, P. Lu, X. Y. Bao, and S. Larochelle, "Multi-parameter sensing based on the stimulated Brillouin scattering of higher-order acoustic modes in OAM fiber," in *Proceedings of the 24th International Conference on Optical Fibre Sensors*, vol. 9634, Article ID 96340L, Curitiba, Brazil, October 2015.

[27] L. W. Sheng, D. X. Ba, and Z. W. Lu, "High-gain and low-distortion Brillouin amplification based on pump multi-frequency intensity modulation," *Chinese Physics B*, vol. 28, no. 1, Article ID 024212, 2019.

[28] W. Jin, W. C. Michie, G. Thursby, M. Konstantaki, and B. Culshaw, "Simultaneous measurement of strain and temperature: error analysis," *Optical Engineering*, vol. 36, no. 2, pp. 598–609, 1997.

[29] Q. Bai, B. Xue, H. Gu et al., "Enhancing the SNR of BOTDR by gain-switched modulation," *Institute of Electrical and Electronics Engineers Photonics Technology Letters*, vol. 31, no. 4, pp. 283–286, 2019.